Biosensors and Bioelectronics 185 (2021) 113281

Contents lists available at ScienceDirect

Biosensors and Bioelectronics

journal homepage: www.elsevier.com/locate/bios

Target-induced transcription amplification to trigger the trans-cleavage activity of CRISPR/Cas13a (TITAC-Cas) for detection of alkaline phosphatase

Xianfeng Wang [a,1], Shiying Zhou [a,1], Chengxiang Chu [a], Mei Yang [a], Danqun Huo [a,b,**], Changjun Hou [a,b,*]

[a] Key Laboratory for Biorheological Science and Technology of Ministry of Education, State and Local Joint Engineering Laboratory for Vascular Implants, Bioengineering College of Chongqing University, Chongqing, 400044, PR China

[b] Chongqing Key Laboratory of Bio-perception & Intelligent Information Processing, School of Microelectronics and Communication Engineering, Chongqing University, Chongqing, 400044, PR China

ARTICLE INFO

Keywords:
Alkaline phosphatase
CRISPR/Cas13a
Fluorescence detection
Biosensor
Transcription

ABSTRACT

Herein, an ultra-sensitive alkaline phosphatase (ALP) sensing strategy is developed by target-induced transcription amplification to trigger the trans-cleavage activity of Cas13a (TITAC-Cas). A double-stranded DNA duplex integrating a T7 promoter with 5′-phosphate and a transcription template (5′P-dsDNA) serves as the ALP substrate. In the absence of ALP, 5′P-dsDNA can be degraded by the λexo, leading to the subsequent transcription failure. In the presence of ALP, dephosphorylation reaction converts the 5′P-dsDNA to 5′OH-dsDNA and provides the protection for T7 promoter against the λexo-digestion. The intact T7 promoter of 5′OH-dsDNA can activate T7 transcription to produce a mass of single-stranded RNA (ssRNA). The ssRNA products possess a full complementarity to the spacer of crRNA and activate the ssRNase activity of CRISPR/Cas13a. As a result, Cas13a exhibits the indiscriminate cleavage of collateral FQ-reporter to release significant fluorescence signal, realizing the ultra-sensitive detection of ALP. Due to the triple signal amplification (ALP self-catalysis, T7 transcription amplification, and trans-cleavage of CRISPR/Cas13a), TITAC-Cas assay shows the ultra-sensitive detection of ALP activity with a wide linear range from 0.008 to 250 $U \cdot L^{-1}$). The LOD is calculated to be 6 ± 0.52 $mU \cdot L^{-1}$. TITAC-Cas assay is also successfully applied for analysis of ALP activity in HepG2 cell lysate with high fidelity. In addition, this method is employed to screen ALP inhibitor.

1. Introduction

Alkaline phosphatase (ALP) is a phosphate-cleaving enzyme existing in various tissues or biofluids, which possesses the responsibility for removal of phosphate under basic conditions (Dong et al., 2015). ALP plays the important roles in living organisms by promoting the dephosphorylation of various substrates and impelling the digestion and absorption of calcium and phosphorus (Coleman, 1992; Giannini et al., 2005). Generally, serum ALP level ranges from 20–140 $U \cdot L^{-1}$ in normal adults, which presents the slightly enhancement in infants and pregnant women (Mahato et al., 2020). The high ALP level (higher than 190 $U \cdot L^{-1}$) in human body may induce many diseases including hypophosphatasia, hepatobiliary diseases and bone diseases, and various cancers (Chen et al. 2017, 2019a). The abnormally low ALP level may cause hematological diseases such as Wilson's disease, anemia and leukemia (Tang et al., 2019). At the same time, neonatal necrotizing enterocolitis is also associated with the decreased levels of ALP activity (Davidson et al., 2019). Therefore, ALP has been deemed as an important biomarker for diagnostics and a potential prognostic indicator. Furthermore, ALP with low activity in saliva (average 5.04 ± 1.866

* Corresponding author. Key Laboratory for Biorheological Science and Technology of Ministry of Education, State and Local Joint Engineering Laboratory for Vascular Implants, Bioengineering College of Chongqing University, Chongqing, 400044, PR China.

** Corresponding author. Key Laboratory for Biorheological Science and Technology of Ministry of Education, State and Local Joint Engineering Laboratory for Vascular Implants, Bioengineering College of Chongqing University, Chongqing, 400044, PR China.

E-mail addresses: huodq@cqu.edu.cn (D. Huo), houcj@cqu.edu.cn (C. Hou).

[1] Xianfeng Wang and Shiying Zhou contributed equally to this work.

https://doi.org/10.1016/j.bios.2021.113281
Received 6 February 2021; Received in revised form 13 April 2021; Accepted 21 April 2021
Available online 27 April 2021

$U \cdot L^{-1}$) (Jazaeri et al., 2015), urine (Amador et al., 1963), cerebrospinal fluid (Guzowski and Knobloch, 1963) and synovial fluid (Lehman et al., 1964) can be measured to elucidate the physiological or pathological processes in human body. In addition, ALP activity is used internationally to evaluate the pasteurization effect of raw milk. The ALP activity over 0.35 $U \cdot L^{-1}$ indicates that the microbial content in the milk exceeds the standard (Rankin et al., 2010). Most conventional methods cannot meet the detection requirements of this low abundance of ALP. Consequently, development of reliable, sensitive, simple and low-cost assay for precise monitoring ALP activity fully exhibits the clinical significance.

In recent past, several conventional methods based on gel electrophoresis (Benham et al., 1978), electrochemistry (Mahato et al., 2020), colorimetry (Chen et al., 2019a; Yang et al., 2020), SERS (Ingram et al., 2009) and fluorescence (Jie et al., 2019; Ke et al., 2020; Xu et al., 2020) have been established to measure ALP activity. However, the strategies based on gel electrophoresis just present the semi-quantitative analysis. Electrochemical methods involve in the time-consuming detection, and the complex modification and washing of electrode. The SERS-based strategies surfer from the requirements of sophisticated and expensive equipment. The colorimetric methods are usually limited to their poor sensitivity. Alternatively, fluorescent assays are frequently applied for detection of ALP activity because of their superiorities in high sensitivity, simple operations, easy integration and readout. And various fluorescent nanomaterials and chemical probes have been used to develop fluorescent assays for sensing. Nevertheless, the nanomaterial-based sensors suffer from the complex steps for the synthesis and modification of functionalized nanomaterials, such as quantum dots (Ke et al., 2020) and precious metal nanocluster (Ni et al., 2019; Wang et al., 2020b). The fluorescence sensors based on synthetic chemical probe also display the requirements of complex synthesis, such as aggregation-induced emission (AIE) probe (Li et al., 2019b; Zhang et al., 2020) and two-photon fluorescent probe (Zhang et al., 2017). To make matters worse, these strategies are usually interfered by other irrelevant interferents and apt to present responses to other phosphatases. Therefore, it is extremely needed to establish more reliable, accurate, and sensitive strategies for determination of ALP activity.

Among different amplification strategies, polymerase-based DNA/RNA amplification provides a more simple and effective method for signal amplification, which can be classified as DNA polymerase-catalytic extension and RNA polymerase-catalytic transcription amplifications. Nevertheless, in most cases, the non-nucleic acid molecules (such as adenosine triphosphate (ATP) (Song et al., 2018), pyrophosphate (PPi) (Hou et al., 2019), L-ascorbic acid 2-phosphate sesquimagnesium salt hydrate (AAP) (Wang et al., 2018) and p-nitrophenylphosphate (PNPP) (Li et al., 2016)) serve as the ALP substrates, which cannot be used for polymerase-based DNA/RNA amplification. In previous studies, DNA substrates have been demonstrated for ALP detection. Nevertheless, none of them integrated in DNA/RNA-mediated amplification because of the limitation of effective signal conversion and detection strategies (Jiao et al., 2014; Zhang et al., 2015). In addition, several DNA polymerase-based strategies have been combined with molecular beacon or hairpin probe for ALP detection. However, polymerase just presents the DNA extension to switch on the molecular beacon or hairpin probe (Ma, 2012; Zhang et al., 2015), which makes no efforts for the improvement of nucleic acid amplification. Therefore, it is a meaningful attempt to apply nucleic acid amplification to obtain significant signal amplification for measurement of ALP activity.

Recently, the discoveries of RNA-guided adaptive CRISPR/Cas system have exhibited the powerful promise in the detection of nucleic acid (Chen et al., 2018b; Gootenberg et al., 2017). More importantly, the Cas12a, Cas12b, Cas13a, and Cas14 show the non-specific degradation of surrounding single-stranded DNA or RNA (referred as trans-cleavage) after the specific recognition of target nucleic acids (Li et al., 2019a). The trans-cleavage activity of Cas enzyme can be used for digestion of collateral FQ-reporter (a short ssRNA or DNA labeled with 5′-FAM and 3′-BHQ1) with a high speed of thousands of turnovers per second, which makes CRISPR/Cas systems possess the self-signal amplification and signal reporting. CRISPR/Cas itself is a signal amplification system. The combination of CRISPR/Cas with other amplification method can easily realize the cascade amplification, ensuring the outstanding sensitivity of detection. Simultaneously, the integration of CRISPR/Cas in sensing and actuating properties simplifies the design of the biosensing system (Li et al., 2019a). Compared with conventional probes for nucleic acid recognition, CRISPR/Cas provides a two-part recognition mode based on Cas effector and the guide RNA. Only target sequence and crRNA complement each other to activate the Cas activity. Consequently, this two-part recognition mode provides more excellent selectivity of CRISPR/Cas compared with conventional nucleic acid probes (Bonini et al., 2021). In view of the programmability of crRNA and the characteristic of biological target, just by designing different transcription-initiating mechanisms and changing the spacer sequence of crRNA, CRISPR/Cas can prove to be a versatile tool for sensing of any nucleic acids or non-nucleic acid targets (Shen et al., 2020; Wang et al. 2020a, 2020c; Zhao et al., 2020). Currently, several CRISPR/Cas-based detection platforms including Cas12-based HOLMES (Li et al., 2018), Cas13-based SHERLOCK (Gootenberg et al., 2018), and Cas12/Cas14-based DETECTR (Chen et al., 2018b; Harrington et al., 2018), have been established for sensing of viruses (especially for COVID-19 diagnosis) (Huang et al., 2020), and single nucleotide polymorphism (SNP) (Teng et al., 2019). Most of these CRISPR/Cas sensors concentrate on the detection of nucleic acids with the challenge for detection of non-nucleic-acid targets. As the attempts for exploration, Lu and Liu's group propose the functional DNA (fDNA) to respond with the non-nucleic acid target (Dai et al., 2019; Xiong et al., 2020), which further regulates the cleavage activity of CRISPR/Cas for signal transduction. The innovative application of fDNA (like aptamer or RNA-cleaving DNAzyme) obviously expands the CRISPR/Cas sensors for detection of non-nucleic-acid targets including small molecules, metal ions and proteins. However, the fDNA-based CRISPR/Cas sensors just present the direct recognition without further target amplification, resulting that detecting low-abundance non-nucleic-acid targets is still elusive. For biomaker detection, sensitivity is a key parameter. Therefore, it is meaningful to use CRISPR/Cas system for determination of ALP activity to obtain the sufficient signal amplification with high selectivity and low back ground.

Herein, we present a triple signal amplification (TITAC-Cas) on the base of dephosphorylation-activated transcription amplification-mediated CRISPR/Cas13a system for ultra-sensitive measurement of ALP activity, which successfully broadens the applications of CRISPR/Cas13a-based sensors for analysis of biological enzymes. In this work, T7 promoter/template DNA duplex with 5′-phosphate in T7 promoter serves as the ALP substrate. ALP-dephosphorylation provides the protection for T7 promoter (5′-hydroxyl)/template DNA against the digestion from λexo. The intact substrate DNA executes the T7 transcription to generate a mass of ssRNA, which serves as the activator to unlock the ssRNase activity of Cas13a, leading to the degradation of FQ-reporter to release the sufficient fluorescence signal. With such a design, TITAC-Cas assay with triple signal amplification enables the detection of ALP activity with ultra-sensitivity and extremely low background. These triple signal amplification steps are performed in an isothermal manner and the detection process can be finished within 100 min, showing the rapid and facile measurement of ALP activity. In addition, the TITAC-Cas assay is not only successfully applied for analysis the ALP activity in HepG2 cell extracts, but also exhibits the capacity of screening enzyme inhibitor and evaluating its inhibition efficiency.

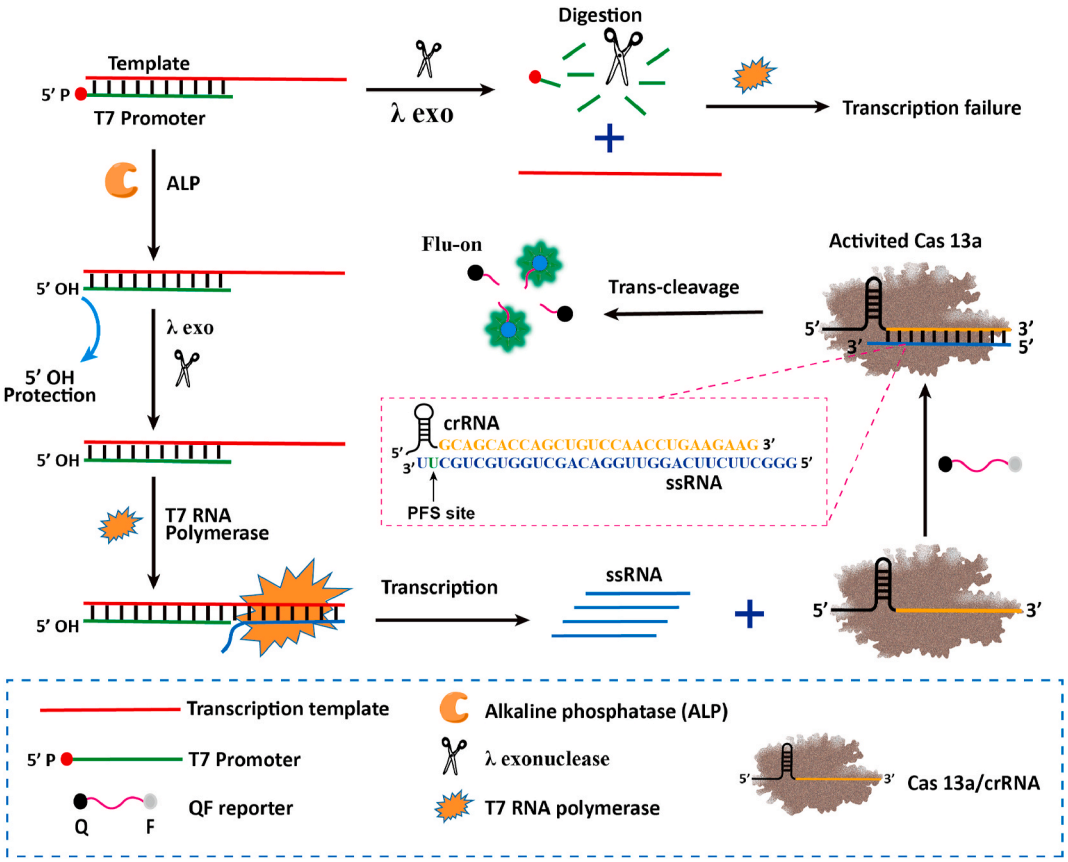

Scheme 1. Schematic illustration of target-induced transcription amplification to trigger the trans-cleavage activity of CRISPR/Cas13a (TITAC-Cas) for detection of ALP activity.

2. Experimental section

2.1. Reagents and instruments

LwCas13a was purchased from Kexin biotechnology Co., Ltd (Beijing, China). Lambda exonuclease (λexo), T7 RNA synthesis Kit, T7 RNA polymerase, rNTP were purchased from NEB Co., Ltd (Beijing, China). miRNA purification kit was ordered from TIANGEN Biotechnology (Beijing, China). Nucleic acid dye was obtained from TSINGKE (Beijing, China). Alkaline phosphatase (ALP), sodium orthovanadate (V) dodecahydrate (Na_3VO_4), acryl/bis 30% solution (29:1), ammonium persulfate (APS), peroxidase (HRP), glucose oxidase (GO), BSA, streptavidin (SA), TBE buffer, TE buffer, DNA marker, PAGE-related reagents, 6 × loading buffer, ddH_2O, DEPC-treated water, and the oligonucleotides used in this work were obtained from Sangon Biotechnology (Shanghai, China). The fluorescence spectra were recorded on a fluorescence spectrometer (PerkinElmer). The DNA sequences used in this work are shown in Table S1.

2.2. Preparation of crRNA

crRNA used in this work was synthetized via a T7 transcription. DNA transcription template was obtained by the hybridization of T7-crRNA-F (10 μM) and T7 promoter (10 μM) via a denaturation (95 °C for 3 min) and an annealing process to 25 °C. After that, 18 μL transcription template, 10 μL NTP buffer mix (20 mM), and 2 μL T7 RNA polymerase were fully mixed and incubated at 37 °C for 16 h. Then 3 μL of DNase I and 3.5 μL DNase I buffer were added and reacted at 37 °C for 1 h to degrade the DNA template. crRNA was purified with a miRNA purification kit and quantified with a NanoDrop 2000C (Thermo Fisher). The final crRNA was identified by gel electrophoresis analysis (Fig. S1).

2.3. Dephosphorylation of T7 promoter

A mixture containing T7 promoter with 5′-phosphate (1 μM) and ALP-template (1 μM) in 10 mM Tris-HCl (pH 8) was heated at 95 °C for 5 min and slowly cooled down to 20 °C with the speed of 0.1 °C/min to obtain proximity complex of T7 promoter/template duplex. Dephosphorylation was performed in 20 μL of reaction mixture containing 14 μL ddH_2O, 2 μL of 10 × cutsmart buffer, 2 μL of proximity complex, and 2 μL of ALP with different concentrations, and reacted at 37 °C for 40 min, followed by inactivation at 65 °C for 10 min to terminate dephosphorylation. After that, 1 U of λexo was added in the mixture and reacted at 37 °C for 30 min. Subsequently, the incubation at 90 °C for 5 min was performed to terminate the digestion of T7 promoter.

2.4. Measurement of ALP activity using TITAC-Cas assay

ALP activity detection progress involves in the T7 transcription and the recognition of CRISPR/Cas13a system. 6 μL of λexo digestion products, 2 μL of 10 × NEBuffer 2.1, 2 U RNase inhibitor, 0.5 μL of T7 RNA polymerase (50 U/μL) and 1 μL of rNTP (20 mM) were added in 10 μL ddH_2O. The mixture was reacted at 37 °C for 60 min to obtain a mass of ssRNA. For CRISPR/Cas13a detection, 2 μL of transcription products, 2 μL of crRNA (2 μM), 2 μL of LwCas13a (0.5 μM), 2 U RNase inhibitor, 1 μL of FQ-reporter (10 μM), 2 μL of 10 × NEBuffer 2.1 were added in 10 μL ddH_2O. The cleavage of CRISPR/Cas13a was performed at 37 °C for 25 min. Then 80 μL ddH_2O was added in above mixture. The fluorescence spectra of tested samples were recorded after the excitation of 480 nm. The excitation and emission slits were set as 12 nm and 7 nm, respectively. The fluorescence intensity at 520 nm was applied for quantification of ALP.

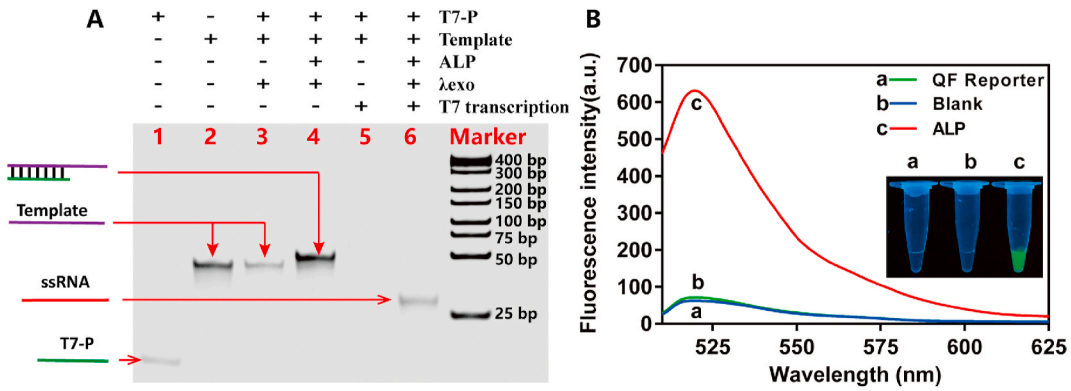

Fig. 1. (A) Polyacrylamide gel electrophoresis (PAGE) analysis of TITAC-Cas sensing system. Lane 1: 5′P-T7 promoter; lane 2: ALP-template; lane 3: λexo digestion of 5′P-T7 promoter/template duplex in the absence of ALP; lane 4: λexo digestion of T7 promoter/template duplex in the presence of ALP; lane 5: T7 transcription (without ALP); lane 6: T7 transcription (with ALP). (B) Fluorescence spectra induced by different samples: (a) FQ-reporter; (b) crRNA/Cas13a + FQ-reporter + transcription products (without ALP); (c) crRNA/Cas13a + FQ-reporter + transcription products (with ALP).

2.5. Gel electrophoresis

The dephosphorylation and transcription products was analyzed by a 15% nondenaturing polyacrylamide gel electrophoresis. The test sample in 1 × loading buffer was added into the lane of gel. Electrophoresis was performed in 1 × TBE buffer at 100 V for 70 min. The final gel was dyed by 1 × TS-GelRed for 15 min and photographed by a JENA UVsolo Imager.

2.6. Cell culture and preparation of cell extracts

Human hepatocellular liver carcinoma cell line (HepG2 cell) and human umbilical vein endothelial cells (HUVEC cell) were cultured in DMEM/F-12 (Hyclone, USA) supplemented with 10% fetal bovine serum (Solarbio, China) and 1% penicillin-streptomycin solution, and then maintained at 37 °C in 5% CO_2 of humid atmosphere. The cells were collected by trypsinization then centrifugated (3 min, 1000 rpm) and re-suspended into PBS (0.01 M, pH 7.4) solution. The number of cells was identified by hemocytometer. The cell suspension was centrifuged to discard the supernatant, and then the cell sediment was collected and re-suspended in 200 μL RIPA lysis buffer (10 mM Tris-HCl, 150 mM NaCl, 1% NP-40, 0.25 mM sodium deoxycholate) and placed on ice for 30 min. The cell extracts were obtained by centrifugated at 12,000 rpm for 20 min at 4 °C and then stored at −80 °C for further use.

3. Results and discussion

3.1. Design of TITAC-Cas sensing system

In this work, we propose a target-induced transcription amplification to trigger the trans-cleavage activity of cas13a (referred as "TITAC-Cas") for ultra-sensitive analysis of ALP activity. In most cases, DNA polymerase-based amplification strategies are used for measurement of ALP activity due to the high signal amplification efficiency. However, it suffers from the nonspecific amplification induced by the template/primer-independent DNA extension, which always involves in a strong background signal. Signal amplification based on T7 RNA polymerase presents the accurately T7 promoter-dependent transcription and executes RNA transcription just in the existence of intact T7 promoter, which avoids nonspecific amplification. The principle of TITAC-Cas assay for measurement of ALP activity is revealed in Scheme 1, which involves in triple signal amplification. T7 promoter (green sequence) with 5′-phosphate can bind with 3′-terminus of the template (red sequence) to form the T7 promoter/template duplex. Without ALP, T7 promoter with 5′-phosphate in proximity duplex was completely digested by λexo, which can selectively degrade 5′-phosphated DAN from 5′ to 3′ direction with the speed of 12 nt/s, leaving the ALP-template intact. Due to the promoter-dependency of T7 RNA polymerase, the absence of ALP makes the result of the transcription failure. Contrarily, ALP-dephosphorylation provides the conversion from 5′-phosphate in T7 sequence to 5′-hydroxyl (the first signal amplification), which protects T7 promoter/template duplex from being digested by λexo. The intact T7 promoter/template duplex executes the subsequent T7 transcription to generate a mass of ssRNA (the second amplification).

Afterward, CRISPR/Cas13a measurement is achieved via crRNA-guided ssRNA recognition inducing the trans-cleavage activity of LwCas13a. First, crRNA containing a 36 nt repeat sequence (black domain with hairpin structure) and a 28 nt programmable spacer region (yellow sequence) binds with LwCas13a to form the CRISPR/Cas13a system. crRNA-assembly can guide LwaCas13a to search and recognize the ssRNA with a complementary sequence (blue sequence) of the spacer region of crRNA to form the ternary hybrid of crRNA/ssRNA/Cas13a. In addition, a protospacer flanking site (PFS, the U base with green color) is designed in ssRNA sequence. In this case, ssRNA binding activates two conserved higher eukaryote and prokaryote nucleotide binding (HEPN) regions of LwCas13a to unlock the ssRNase activity, resulting in the indiscriminate cleavage of collateral FQ-reporter with thousands of turnovers per second to release fluorescence signal (the third amplification). Therefore, by integrating the target-induced transcription amplification and CRISPR/Cas13a system, significant signal amplification is achieved for ultra-sensitive measurement of ALP activity with insignificant background signal.

3.2. Feasibility of TITAC-Cas assay for measurement of ALP activity

The strategy on the base of ALP-mediated protection of T7 promoter to induce transcription amplification was verified by 15% non-denaturating PAGE. As can be seen from Fig. 1A, T7 promoter and ALP-template exhibit obvious single band (lane 1 and 2). Compared with T7 promoter, ALP-template shows a lower electrophoretic mobility due to the longer strand of ALP-template. After λexo digestion without ALP, the band of T7 promoter/template duplex is not observed in lane 3, while an obvious single band displays the same position with ALP-template. It indicates that T7 promoter with 5′-phosphate is completely digested by λexo and leave the ALP-template intact. In contrast, a distinct band with a lower electrophoretic mobility in lane 4 after digestion of λexo in the presence ALP, which is corresponding to the T7 promoter/template duplex. It demonstrates that ALP provides the protection of T7 promoter against the digestion of λexo via the conversion from 5' -phosphate to 5′-hydroxyl, resulting in the complete T7 promoter/template duplex. Subsequently, the band in lane 6 possesses a higher electrophoretic mobility than that of ALP-template and T7

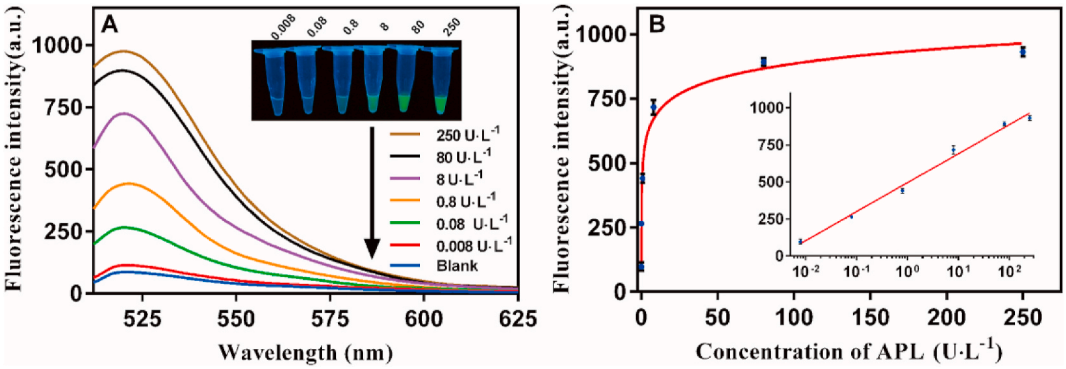

Fig. 2. Detection performances of TITAC-Cas assay for ALP activity. (A) Fluorescence spectra of TITAC-Cas assay induced by different activities of ALP (0.008, 0.08, 0.8, 8, 80, and 250 $U \cdot L^{-1}$). (B) The fluorescence response with ALP activities and corresponding calibration curve (insert in Fig. 2B) between fluorescence response and the logarithmic of ALP activity.

promoter/template duplex, which is deemed as the final ssRNA products after T7 transcription. However, no band is observed in lane 5. These results indicate the feasibility of ALP-mediated protection of T7 promoter to induce transcription amplification. To verify the crRNA-guided ssRNA recognition of CRISPR/Cas13a system for signal amplification, transcription products and FQ-reporter were incubated with crRNA/Cas13a, and the fluorescence intensity were recorded after the excitation of 480 nm. As shown in Fig. 1B, only the presence of ALP induces a significant fluorescence enhancement. It suggests that ALP protects the T7 promoter/template duplex against the λexo digestion and subsequently induces the ssRNA generation to unlock the ssRNase activity of LwCas13a, resulting the degradation of FQ-reporter to release fluorescence signal.

3.3. Optimization of the detection conditions

To achieve the ideal performances of TITAC-Cas assay, detection conditions including dephosphorylation time, concentration of λexo, transcription time, and CRISPR/Cas13a cleavage time were investigated. The ratio of F/F_0 was applied for evaluation of the detection performances, where F represents the fluorescence intensity induced by ALP with the concentration of 8 $U \cdot L^{-1}$, and F_0 represents the fluorescence intensity without ALP. As can be seen from Fig. S2A, the F/F_0 value enhances with the dephosphorylation time change from 10 min to 40 min. After that, negligible enhancement appears over 40 min. It may result from the complete inactivation of ALP or the complete dephosphorylation of 5′-phosphate in T7 promoter substrates after 40 min incubation. Thus 40 min is selected as the optimal time for ALP dephosphorylation. Fig. S2B reveals that the F/F_0 value increases with the gcrowing λexo concentration from 0.01 to 0.05 $U \cdot \mu L^{-1}$, after which a clear decline is observed. It may be interpreted as that low concentration of λexo leads the incomplete digestion of 5′P-T7 promoter to produce the high background. At this case, it reduces the fluorescence difference between experimental group and blank, resulting in the narrow detection range. Generally, λexo exhibits the preferred digestion of dsDNA with 5′-phosphate, but it still provides the slow digestion for non-phosphated substrates, which declines the detection signal intensity and also leads to a relatively narrow sensing range. Therefore, 0.05 $U \cdot \mu L^{-1}$ of λexo is chosen for the following-up experiments. Fig. S2C shows that the F/F_0 value depicts a first increase and then decline, and reaches the maximum upon the transcription for 60 min, which is selected for subsequent researches. For the cleavage of CRISPR/Cas13a

Table 1
Comparison with other methods for ALP activity detection.

Strategy	Signal amplification	Detection range ($U \cdot L^{-1}$)	LOD ($U \cdot L^{-1}$)	Target	Detection time	Ref.
Electrochemisty	SAM/GA/Tris/anti-ALP	0.03–0.3	0.4	/	~8.5 h	Mintz Hemed et al. (2018)
Electrochemisty	SPCE/AuNPs/Au-nano-Dendroids/GO/anti-ALP	100–1000	9.1	Human serum	60 min	Mahato et al. (2020)
Electrochemisty	ALP-responsive anodic ECL of CdSe	2–25	2	Spiked human serum	/	Jiang and Wang (2012)
SERS	ALP catalysis of BCIP and NBA/GNSs substrate	1–10^4	1	/	3 min	Dong et al. (2014)
Colorimetry	PO_4^{3-}-inhibited catalytic activity of Ce(IV)	0–250	2.3	Human serum	40 min	Song et al. (2018)
Colorimetry	Etching of gold/silver core/shell nanorod	5–100	3.3	Human Serum	240 min	Gao et al. (2014)
Colorimetry	Upconversion-based IFE-MRECAmp	0.08–70	0.032	Spiked human serum	66 min	Chen et al. (2019b)
Colorimetry	ALP-regulated formation of PBNPs probe	0.5–16	0.048	Spiked human serum	~100 min	Wei et al. (2021)
Fluorescence	DHXP lighted up by ALP-dephosphorylation	1–100	0.07	HeLa cells	~28 h	Tan et al. (2017)
Fluorescence	Dephosphorylation-initiated TdT amplification	0.1–3	/	Spiked human serum	~240 min	Hu et al. (2017)
Fluorescence	T-Hg(II)-T generated by TdT	0.025–2500	0.025	MCF-7 lysates	190 min	Wang et al. (2019)
Fluorescence	Excited-SIPT and AIE	0–150	0.15	Fetal bovine serum	60 min	Liang et al. (2013)
Fluorescence	PET-induced quenching of APBA-Au NCs	0.02–2.0	0.005	Spiked human serum	50 min	
Fluorescence	CQDs-Ce^{3+}-ATP	4.6–383.3	1.4	Human Serum	120 min	Qian et al. (2015)
Fluorescence	p-nitrophenyl phosphate-Ce^{3+}-calcein	0.4–1.2	0.023	/	~12 h	Chen et al. (2018a)
Fluorescence	ALP-dephosphorylation-initiated transcription amplification-mediated CRISPR/Cas13a	0.008–250	0.006	HepG2 cells	100 min	This work

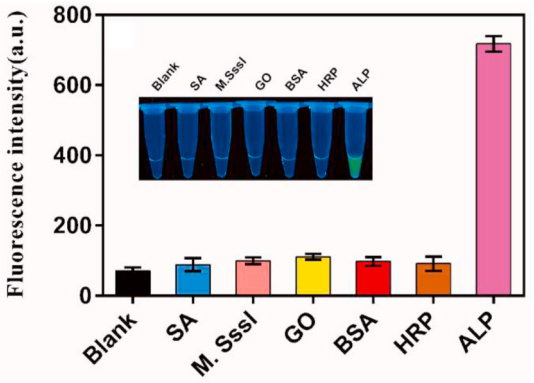

Fig. 3. The fluorescence response of TITAC-Cas assay towards different interferents (M. SssI: 10 U·L^{-1}; GO: 10 mg L^{-1}; SA: 10 mg L^{-1}; BSA: 10 mg L^{-1}; HRP: 10 mg L^{-1}; ALP: 8 U·L^{-1}). Insert: photograph of test sample under ultraviolet radiation (error bars: SD, n = 3).

system, the F/F$_0$ value increases with the time change from 5 to 25 min (Fig. S2D). After that, a decline in F/F$_0$ value is observed, which may result from the nonspecific recognition of CRISPR/Cas13a system with the time prolongation. Therefore, 25 min is selected as the optimal cleavage time for detection of ALP activity.

3.4. Detection performances of TITAC-Cas assay

The detection performances of TITAC-Cas assay were performed by measuring the fluorescence response to different concentrations of ALP. As can be seen from Fig. 2A, the fluorescence signal at 520 nm increases with the growing activity of ALP, suggesting the ALP activity-dependent cleavage of CRISPR/Cas13a for FQ-reporter. Notably, the fluorescence signal shows a linear dependence to the logarithm of ALP activity from 0.008 to 250 U·L^{-1} (Fig. 2B). The regression equation is described as F = 195.6 × lgC +494.8 (R^2 = 0.9887) with the LOD of 6 ± 0.52 mU·L^{-1}, where F represents the fluorescence signal and C represents the activity of ALP. To evaluate the stability of TITAC-Cas assay, 5 samples with the same concentration of ALP (5 U·L^{-1}) were repeatedly measured three times. The relative standard deviation (RSD) of 5 samples is calculated to be 5.72%, indicating TITAC-Cas assay has a good stability (Fig. S3). Compared with other methods with one or two-stage signal amplification signal amplification listed in Table 1, TITAC-Cas assay possesses the obvious advantages in sensitivity. For actual detection limit, the sensitivity of TITAC-Cas assay is about 120-fold higher than the strategy with one-stage signal amplification (Tan et al., 2017) and about 12-fold higher than the assay with dual signal amplification (Hu et al., 2017). These outstanding performances can result from the following aspects: (1) low background signal from the complete digestion of superfluous T7 promoter with 5′-phosphate by λexo; (2) the highly efficient T7 polymerase-based transcription; (3) the powerful trans-cleavage and recognition of CRISPR/Cas13a system for signal amplification. More importantly, the TITAC-Cas assay has the potential to be a universal detection platform. According to the characteristic of biological target, different functional DNA segment with 5′-phosphate can be integrated into the dsDNA hybridization probe to change transcription-initiating mechanisms for more target detection. For instance, with the adjunction of binding site with 5′-phosphate into dsDNA hybridization probe, TITAC-Cas assay can be employed for detection of other kind of DNA binding protein like growth factor-BB. And the adjunction of 5′P-catalytic-site of bio-enzyme leads TITAC-Cas assay possess the capability for detection of other bio-enzymes (e.g. methyltransferase and various endonuclease).

To determine the specificity of the this method for analysis ALP activity, several possible interferents including CpG methyltransferase (M. SssI), BSA, glucose oxidase (GO), streptavidin (SA) and horseradish peroxidase (HRP) were tested by TITAC-Cas assay. As shown in Fig. 3 and Fig. S4, the interferents induce the negligible fluorescence enhancement and exhibit the coincident fluorescence intensity with that of blank sample. In contrast, the presence of ALP leads to a dramatic fluorescence signal enhancement (the red curve and the purple column) and a bright green emission (inset image), demonstrating the outstanding selectivity of TITAC-Cas assay for detection of ALP activity. The superior selectivity results from the specific ALP-dephosphorylation, the specific digestion of dsDNA with 5′-phosphate, and the crRNA-guided ssRNA recognition of CRISPR/Cas13a system.

3.5. ALP inhibitor investigation

It is of great significance to investigate the inhibitor of enzyme in drug design. Except for the application for detection of ALP activity, the TITAC-Cas assay was also employed to screen the potential ALP inhibitors and investigate the interaction mechanism between ALP and its inhibitors. Herein, Na_3VO_4 as a reversible and competitive inhibitor was applied for the inhibition assay. According to the results presented in Fig. 4A, the relative activity of ALP exhibits the rapid concentration-dependent reduction with the increasing concentrations of Na_3VO_4 from 1 to 120 μM. The half maximal inhibitory concentration (IC_{50}) was applied to evaluate the inhibition efficiency of Na_3VO_4, which represents the concentration of an inhibitor needed to obtain 50% of inhibition efficiency. According to the data in Fig. 4A, the IC_{50} of Na_3VO_4 for ALP is calculated to be 18.21 μM. These results indicate that the TITAC-Cas assay not only realizes the determination of ALP activity but also possesses the capacity of screening the inhibitor of ALP.

The TITAC-Cas assay was further used to detect endogenous ALP in

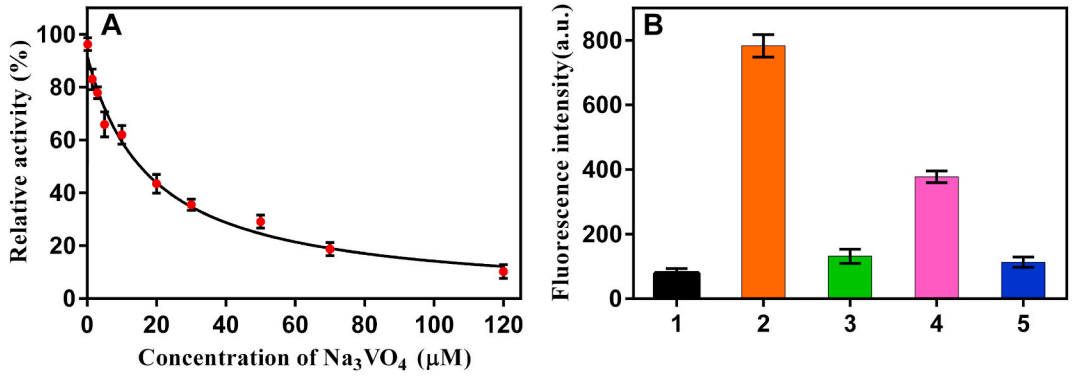

Fig. 4. (A) The reactive activity of ALP (8 U ·L^{-1}) in the presence of different concentration Na_3VO_4. (B) The fluorescence response of TITAC-Cas assay towards different sample in cell inhibition test (1: control sample; 2: 10^4 HepG2 cells; 3: 10^4 HepG2 cells + 150 μM Na_3VO_4; 4: 10^4 HUVEC cells; 5: 10^4 HUVEC cells + 150 μM Na_3VO_4) (error bars: SD, n = 3).

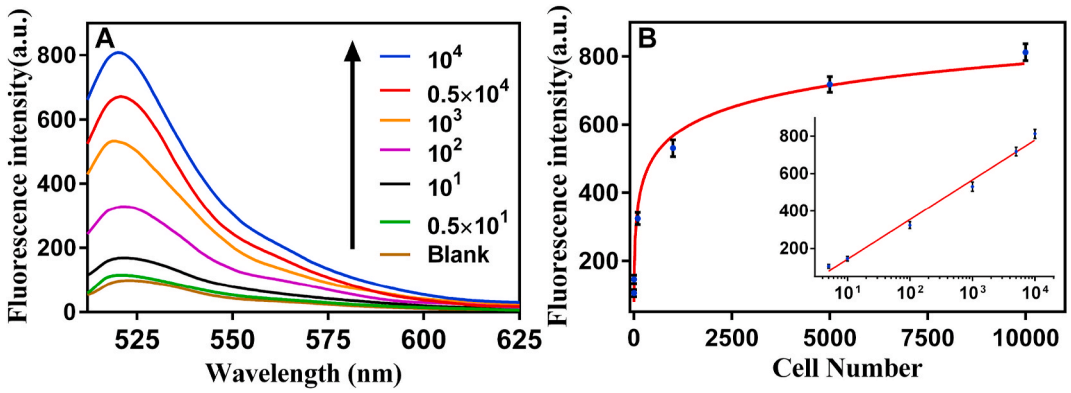

Fig. 5. (A) Fluorescence spectra of TITAC-Cas assay induced by different amount of HepG2 cell. (B) The fluorescence response at 520 nm and corresponding calibration curve towards different HepG2 cell numbers (error bars: SD, n = 3).

human liver cancer HepG2 cell and normal umbilical vein endothelial HUVEC cells (Fig. 4B). Compared with the low back ground signal of control group, the samples with the existence of cell extracts from HepG2 cells and HUVEC cells both induce the significant fluorescence enhancement (column 2 and column 4 in Fig. 4B). Notably, the HepG2 sample exhibits a 2.08-fold higher fluorescence signal than that of HUVEC cells, demonstrating the difference in ALP expression levels in different types of cells. It also indicates the TITAC-Cas assay can be effectively applied for discrimination of ALP activity in cancer tumour cells and normal cells. Importantly, Na_3VO_4 inhibitor exhibits the inhibition effect both in HepG2 cells and HUVEC cells (column 3 and column 5 in Fig. 4B), suggesting that the TITAC-Cas assay can be employed for monitoring of endogenous ALP activity.

3.6. Detection of endogenous ALP activity in HepG2 cell

Moreover, the sensitivity of TITAC-Cas assay for measurement of endogenous ALP activity in HepG2 lysates was investigated. As shown in Fig. 5A, the fluorescence signal enhances with the growing cell numbers, and even 5 cells can also give rise to an obvious distinction with blank sample. A linear correlation is achieved between the fluorescence signal at 520 nm and the logarithm of cell numbers from 5 to 10^4 (Fig. 5B). The corresponding calibration curve is $F = 212 \times lgN - 69.62$ ($R^2 = 0.9872$). All these results demonstrate that the TITAC-Cas assay provides a promising strategy for analysis ALP activity in live cells.

4. Conclusion

In summary, we provide a promising assay based on triple signal amplification (TITAC-Cas assay) for ultra-sensitive and selective measurement of ALP activity in cell lysate. A simple T7 promoter/template duplex with 5′-phosphate in T7 promoter serves as the DNA substrate, which concerts ALP activity signal to amplification signal of RNA transcription. ALP-dephosphorylation provides 5′-hydroxyl to protect T7 promoter/template duplex against the digestion by λexo. T7 transcription converts the dsDNA substrate to ssRNA, which is recognized by CRISPR/Cas13a to cleave the collateral FQ-reporter, releasing sufficient fluorescence signal. This TITAC-Cas assay exhibits the several distinctive advantages. Firstly, the simple ALP-substrate with 5′-phosphate in T7 promoter avoids the laborious preparation of chemical molecule probe. Secondary, T7 transcription amplification is extreme a T7 promoter-dependent process. Therefore, scarce non-specific amplification occurs without ALP, showing extremely low background signal. In addition, owing to the triple signal amplification, the TITAC-Cas assay presents an outstanding sensitivity with the LOD of 6 ± 0.52 $mU \cdot L^{-1}$. Besides, in view of the high sensitivity and outstanding selectivity, TITAC-Cas assay is applied to analyze ALP activity in HepG2 cell. It also exhibits the capacities of enzyme inhibitor screening and inhibitory efficiency estimation, and provides a promising alternative for disease diagnosis or drug screening. The TITAC-Cas assay broadens the applications of CRSIPR/Cas13a for measurement of non-nucleic acid target. In view of the programmability of crRNA and the characteristic of biological target, just by designing different transcription-initiating mechanisms and changing the spacer sequence of crRNA, the TITAC-Cas assay can be extended for analysis of other non-nucleic acid target, such as DNA methyltransferase and DNA-binding proteins.

Declaration of competing interest

The authors declare that they have no known competing financial interests or personal relationships that could have appeared to influence the work reported in this paper.

Acknowledgments

This work was supported by the National Natural Science Foundation of China (NO. 81772290 and 81271930), Graduate Scientific Research and Innovation Foundation of Chongqing, China (Grant NO. CYB20070, 2020CDCGJ014), Fundamental Research Funds for the Central Universities (2019CDYGZD007), The Higher Education Teaching Reform Research Project of Chongqing (203249) and Chongqing Graduate Tutor Team Construction Project.

Appendix A. Supplementary data

Supplementary data to this article can be found online at https://doi.org/10.1016/j.bios.2021.113281.

Credit author statement

All authors who have made substantial contributions to the work are listed in the manuscript. The major experiments and manuscript writing were finished by Xianfeng Wang. Shiying Zhou helped us finish partial cellular experiments. Data analysis of the PAGE electrophoresis was assisted by Chengxiang Chu. Mei Yang provided editing and writing assistance. Danqun Huo and Changjun Hou provided guidance, fund support, instruments and equipment for experiments.

References

Amador, E., Zimmerman, T.S., Wacker, W.E.C., 1963. Urinary alkaline phosphatase activity: I. Elevated urinary LDH and alkaline phosphatase activities for the diagnosis of renal adenocarcinomas. J. Am. Med. Assoc. 185 (10), 769–775.
Benham, F.J., Povey, M.S., Harris, H., 1978. Heterogeneity of alkaline phosphatases in different HeLa lines. Somat. Cell Mol. Genet. 4 (1), 13–25.
Bonini, A., Poma, N., Vivaldi, F., Kirchhain, A., Salvo, P., Bottai, D., Tavanti, A., Di Francesco, F., 2021. Advances in biosensing: the CRISPR/Cas system as a new

powerful tool for the detection of nucleic acids. J. Pharmaceut. Biomed. Anal. 192, 113645.
Chen, C., Zhao, D., Jiang, Y., Ni, P., Zhang, C., Wang, B., Yang, F., Lu, Y., Sun, J., 2019a. Logically regulating peroxidase-like activity of gold nanoclusters for sensing phosphate-containing metabolites and alkaline phosphatase activity. Anal. Chem. 91 (23), 15017–15024.
Chen, C., Zhao, J., Lu, Y., Sun, J., Yang, X., 2018a. Fluorescence immunoassay based on the phosphate-triggered fluorescence turn-on detection of alkaline phosphatase. Anal. Chem. 90 (5), 3505–3511.
Chen, H., Zhou, Z., Lu, Q., Wu, C., Liu, M., Zhang, Y., Yao, S., 2019b. Molecular structure regulation and enzyme cascade signal amplification strategy for upconversion ratiometric luminescent and colorimetric alkaline phosphatase detection. Anal. Chim. Acta 1051, 160–168.
Chen, J.S., Ma, E., Harrington, L.B., Da Costa, M., Tian, X., Palefsky, J.M., Doudna, J.A., 2018b. CRISPR-Cas12a target binding unleashes indiscriminate single-stranded DNase activity. Science 360 (6387), 436–439.
Chen, L., Yang, G., Wu, P., Cai, C., 2017. Real-time fluorescence assay of alkaline phosphatase in living cells using boron-doped graphene quantum dots as fluorophores. Biosens. Bioelectron. 96, 294–299.
Coleman, J.E., 1992. Structure and mechanism of alkaline phosphatase. Annu. Rev. Biophys. Biomol. Struct. 441–483. Annual Reviews Inc.
Dai, Y., Somoza, R.A., Wang, L., Welter, J.F., Li, Y., Caplan, A.I., Liu, C.C., 2019. Exploring the trans-cleavage activity of CRISPR-Cas12a (cpf1) for the development of a universal electrochemical biosensor. Angew. Chem. Int. Ed. 58 (48), 17399–17405.
Davidson, J.A., Urban, T.T., Tong, S., Maddux, A., Hill, G., Frank, B.S., Watson, J.D., Jaggers, J., Simoes, E.A.F., Wischmeyer, P., 2019. Alkaline phosphatase activity and endotoxemia after infant cardiothoracic surgery. Shock 51 (3), 328–336.
Dong, J., Li, Y., Zhang, M., Li, z., Yan, T., Qian, W., 2014. Ultrasensitive surface-enhanced Raman scattering detection of alkaline phosphatase. Anal. Methods 6 (22), 9168–9172.
Dong, L., Miao, Q., Hai, Z., Yuan, Y., Liang, G., 2015. Enzymatic hydrogelation-induced fluorescence turn-off for sensing alkaline phosphatase in vitro and in living cells. Anal. Chem. 87 (13), 6475–6478.
Gao, Z., Deng, K., Wang, X.-D., Miró, M., Tang, D., 2014. High-resolution colorimetric assay for rapid visual readout of phosphatase activity based on gold/silver core/shell nanorod. ACS Appl. Mater. Interfaces 6 (20), 18243–18250.
Giannini, E.G., Testa, R., Savarino, V., 2005. Liver enzyme alteration: a guide for clinicians. CMAJ (Can. Med. Assoc. J.) 172 (3), 367–379.
Gootenberg, J.S., Abudayyeh, O.O., Kellner, M.J., Joung, J., Collins, J.J., Zhang, F., 2018. Multiplexed and portable nucleic acid detection platform with Cas13, Cas12a, and Csm6. Science 360 (6387), 439.
Gootenberg, J.S., Abudayyeh, O.O., Lee, J.W., Essletzbichler, P., Dy, A.J., Joung, J., Verdine, V., Donghia, N., Daringer, N.M., Freije, C.A., Myhrvold, C., Bhattacharyya, R.P., Livny, J., Regev, A., Koonin, E.V., Hung, D.T., Sabeti, P.C., Collins, J.J., Zhang, F., 2017. Nucleic acid detection with CRISPR-Cas13a/C2c2. Science 356 (6336), 438–442.
Guzowski, K., Knobloch, J., 1963. Disorders of the nervous system: activity of acid and alkaline phosphatase in the cerebrospinal fluid. Arch. Neurol. 8 (1), 105–111.
Harrington, L.B., Burstein, D., Chen, J.S., Paez-Espino, D., Ma, E., Witte, I.P., Cofsky, J.C., Kyrpides, N.C., Banfield, J.F., Doudna, J.A., 2018. Programmed DNA destruction by miniature CRISPR-Cas14 enzymes. Science 362 (6416), 839–842.
Hou, L., Qin, Y., Li, J., Qin, S., Huang, Y., Lin, T., Guo, L., Ye, F., Zhao, S., 2019. A ratiometric multicolor fluorescence biosensor for visual detection of alkaline phosphatase activity via a smartphone. Biosens. Bioelectron. 143, 111605.
Hu, Z., Chen, J., Li, Y., Wang, Y., Zhang, Q., Hussain, E., Yang, M., Shahzad, S.A., Yu, D., Yu, C., 2017. Nucleic acid-controlled quantum dots aggregation: a label-free fluorescence turn-on strategy for alkaline phosphatase detection. Talanta 169, 64–69.
Huang, Z., Tian, D., Liu, Y., Lin, Z., Lyon, C.J., Lai, W., Fusco, D., Drouin, A., Yin, X., Hu, T., Ning, B., 2020. Ultra-sensitive and high-throughput CRISPR-powered COVID-19 diagnosis. Biosens. Bioelectron. 164, 112316.
Ingram, A., Moore, B.D., Graham, D., 2009. Simultaneous detection of alkaline phosphatase and β-galactosidase activity using SERRS. Bioorg. Med. Chem. Lett 19 (6), 1569–1571.
Jazaeri, M., Malekzadeh, H., Abdolsamadi, H., Rezaei-Soufi, L., Samami, M., 2015. Relationship between salivary alkaline phosphatase enzyme activity and the concentrations of salivary calcium and phosphate ions. Cell J 17 (1), 159–162.
Jiang, H., Wang, X., 2012. Alkaline phosphatase-responsive anodic electrochemiluminescence of CdSe nanoparticles. Anal. Chem. 84 (16), 6986–6993.
Jiao, H., Chen, J., Li, W., Wang, F., Zhou, H., Li, Y., Yu, C., 2014. Nucleic acid-regulated perylene probe-induced gold nanoparticle aggregation: a new strategy for colorimetric sensing of alkaline phosphatase activity and inhibitor screening. ACS Appl. Mater. Interfaces 6 (3), 1979–1985.
Jie, Z., Qi, G., Xu, C., Jin, Y., 2019. Enzymatic preparation of plasmonic-fluorescent quantum dot-gold hybrid nanoprobes for sensitive detection of glucose and alkaline phosphatase and dual-modality cell imaging. Anal. Chem. 91 (21), 14074–14079.
Ke, C.B., Lu, T.L., Chen, J.L., 2020. Fluorometric determination of amifostine and alkaline phosphatase on amphiprotic molecularly imprinted silica crosslinked with binary functional silanes and carbon dots. Biosens. Bioelectron. 151.
Lehman, M.A., Kream, J., Brogna, D., 1964. Acid and alkaline phosphatase activity in the serum and synovial fluid of patients with arthritis. JBJS 46 (8).
Li, G., Fu, H., Chen, X., Gong, P., Chen, G., Xia, L., Wang, H., You, J., Wu, Y., 2016. Facile and sensitive fluorescence sensing of alkaline phosphatase activity with photoluminescent carbon dots based on inner filter effect. Anal. Chem. 88 (5), 2720–2726.
Li, S.-Y., Cheng, Q.-X., Wang, J.-M., Li, X.-Y., Zhang, Z.-L., Gao, S., Cao, R.-B., Zhao, G.-P., Wang, J., 2018. CRISPR-Cas12a-assisted nucleic acid detection. Cell Discov. 4 (1), 20.
Li, Y., Li, S., Wang, J., Liu, G., 2019a. CRISPR/Cas systems towards next-generation biosensing. Trends Biotechnol. 37 (7), 730–743.
Li, Y., Xie, R., Pang, X., Zhou, Z., Xu, H., Gu, B., Wu, C., Li, H., Zhang, Y., 2019b. Aggregation-induced emission fluorescent probe for monitoring endogenous alkaline phosphatase in living cells. Talanta 205.
Liang, J., Kwok, R.T.K., Shi, H., Tang, B.Z., Liu, B., 2013. Fluorescent light-up probe with aggregation-induced emission characteristics for alkaline phosphatase sensing and activity study. ACS Appl. Mater. Interfaces 5 (17), 8784–8789.
Ma, C., 2012. Highly sensitive detection of alkaline phosphatase using molecular beacon probes based on enzymatic polymerization. Mol. Cell. Probes 26 (3), 113–115.
Mahato, K., Purohit, B., Kumar, A., Chandra, P., 2020. Clinically comparable impedimetric immunosensor for serum alkaline phosphatase detection based on electrochemically engineered Au-nano-Dendroids and graphene oxide nanocomposite. Biosens. Bioelectron. 148, 111815.
Mintz Hemed, N., Convertino, A., Shacham-Diamand, Y., 2018. Alkaline phosphatase detection using electrochemical impedance of anti-alkaline phosphatase antibody (Ab354) functionalized silicon-nanowire-forest in phosphate buffer solution. Sensor. Actuator. B Chem. 259, 809–815.
Ni, P., Chen, C., Jiang, Y., Zhang, C., Wang, B., Cao, B., Li, C., Lu, Y., 2019. Gold nanoclusters-based dual-channel assay for colorimetric and turn-on fluorescent sensing of alkaline phosphatase. Sensor. Actuator. B Chem. 301.
Qian, Z., Chai, L., Tang, C., Huang, Y., Chen, J., Feng, H., 2015. Carbon quantum dots-based recyclable real-time fluorescence assay for alkaline phosphatase with adenosine triphosphate as substrate. Anal. Chem. 87 (5), 2966–2973.
Rankin, S.A., Christiansen, A., Lee, W., Banavara, D.S., Lopez-Hernandez, A., 2010. Invited review: the application of alkaline phosphatase assays for the validation of milk product pasteurization. J. Dairy Sci. 93 (12), 5538–5551.
Shen, J., Zhou, X., Shan, Y., Yue, H., Huang, R., Hu, J., Xing, D., 2020. Sensitive detection of a bacterial pathogen using allosteric probe-initiated catalysis and CRISPR-Cas13a amplification reaction. Nat. Commun. 11 (1), 267.
Song, H., Wang, H., Li, X., Peng, Y., Pan, J., Niu, X., 2018. Sensitive and selective colorimetric detection of alkaline phosphatase activity based on phosphate anion-quenched oxidase-mimicking activity of Ce(IV) ions. Anal. Chim. Acta 1044, 154–161.
Tan, Y., Zhang, L., Man, K.H., Peltier, R., Chen, G., Zhang, H., Zhou, L., Wang, F., Ho, D., Yao, S.Q., Hu, Y., Sun, H., 2017. Reaction-based off–on near-infrared fluorescent probe for imaging alkaline phosphatase activity in living cells and mice. ACS Appl. Mater. Interfaces 9 (8), 6796–6803.
Tang, Z., Chen, H., He, H., Ma, C., 2019. Assays for alkaline phosphatase activity: progress and prospects. Trac. Trends Anal. Chem. 113, 32–43.
Teng, F., Guo, L., Cui, T., Wang, X.-G., Xu, K., Gao, Q., Zhou, Q., Li, W., 2019. CDetection: CRISPR-Cas12b-based DNA detection with sub-attomolar sensitivity and single-base specificity. Genome Biol. 20 (1), 132.
Wang, D.-X., Wang, J., Du, Y.-C., Ma, J.-Y., Wang, S.-Y., Tang, A.-N., Kong, D.-M., 2020a. CRISPR/Cas12a-based dual amplified biosensing system for sensitive and rapid detection of polynucleotide kinase/phosphatase. Biosens. Bioelectron. 168, 112556.
Wang, K., Jiang, L., Zhang, F., Wei, Y., Wang, K., Wang, H., Qi, Z., Liu, S., 2018. Strategy for in situ imaging of cellular alkaline phosphatase activity using gold nanoflower probe and localized surface plasmon resonance technique. Anal. Chem. 90 (23), 14056–14062.
Wang, M., Wang, S., Li, L., Wang, G., Su, X., 2020b. β-Cyclodextrin modified silver nanoclusters for highly sensitive fluorescence sensing and bioimaging of intracellular alkaline phosphatase. Talanta 207.
Wang, X., Chen, X., Chu, C., Deng, Y., Yang, M., Ji, Z., Xu, F., Huo, D., Luo, Y., Hou, C., 2020c. Four-stage signal amplification for trace ATP detection using allosteric probe-conjugated strand displacement and CRISPR/Cpf1 trans-cleavage (ASD-Cpf1). Sensor. Actuator. B Chem. 323.
Wang, Y., Yang, L., Li, N., Sun, C., Xia, Y., Yuan, L., Lu, J., Liu, F., Xing, X., 2019. A versatile assay for alkaline phosphatase detection based on thymine-HgII-thymine structure generation mediated by TdT. Talanta 195, 566–572.
Wei, Y.-Y., Zhang, Y.-Z., Song, D., Li, J., Xu, Z.-R., 2021. Alkaline phosphatase-regulated in situ formation of chromogenic probes for multicolor visual sensing of biomarkers. Talanta 228, 122222.
Xiong, Y., Zhang, J., Yang, Z., Mou, Q., Ma, Y., Xiong, Y., Lu, Y., 2020. Functional DNA regulated CRISPR-Cas12a sensors for point-of-care diagnostics of non-nucleic-acid targets. J. Am. Chem. Soc. 142 (1), 207–213.
Xu, J., Zhang, H., Zhang, W., Li, P., Zhang, W., Wang, H., Tang, B., 2020. Fluorescent nanosensor for: in situ detection of phosphate and alkaline phosphatase in mice with parathyroid dysfunction. Chem. Commun. 56 (16), 2431–2434.
Yang, Q., Wang, X., Peng, H., Arabi, M., Li, J., Xiong, H., Choo, J., Chen, L., 2020. Ratiometric fluorescence and colorimetry dual-mode assay based on manganese dioxide nanosheets for visual detection of alkaline phosphatase activity. Sensor. Actuator. B Chem. 302, 127176.
Zhang, H., Xiao, P., Wong, Y.T., Shen, W., Chhabra, M., Peltier, R., Jiang, Y., He, Y., He, J., Tan, Y., Xie, Y., Ho, D., Lam, Y.W., Sun, J., Sun, H., 2017. Construction of an alkaline phosphatase-specific two-photon probe and its imaging application in living cells and tissues. Biomaterials 140, 220–229.

Zhang, L., Hou, T., Li, H., Li, F., 2015. A highly sensitive homogeneous electrochemical assay for alkaline phosphatase activity based on single molecular beacon-initiated T7 exonuclease-mediated signal amplification. Analyst 140 (12), 4030–4036.
Zhang, X., Ren, C., Hu, F., Gao, Y., Wang, Z., Li, H., Liu, J., Liu, B., Yang, C., 2020. Detection of bacterial alkaline phosphatase activity by enzymatic in situ self-assembly of the AIEgen-peptide conjugate. Anal. Chem. 92 (7), 5185–5190.
Zhao, X., Zeng, L., Mei, Q., Luo, Y., 2020. Allosteric probe-initiated wash-free method for sensitive extracellular vesicle detection through dual cycle-assisted CRISPR-Cas12a. ACS Sens. 5 (7), 2239–2246.